

# Particle dynamics simulation for supersonic heterogeneous flows around an obstacle

Vladimir V. Vinnikov

Dmitry L. Reviznikov  
vvinnikov@list.ru

Andrew V. Sposobin

## Abstract

This paper is concerned with numerical simulation of dispersed phase dynamics in supersonic dusty flows. Admixture equations are solved in Lagrangian variables due to straightforward handling of particle reflections from an obstacle. Two common approaches for particle simulation in path-following variables are discussed, namely: discrete trajectories method and discrete elements method respectively. Both methods yield particle concentrations and other required parameters for storage in arbitrary grids and further processing.

## 1 Introduction

Gas flows with dispersed admixture often occur in various physical processes and technical applications. Flow dynamics gains new qualities and shows new effects with the introduction of dispersed particles. New effects include compaction of a shock layer, intensification of convective heat flux to an obstacle surface, erosion of the exposed surface and screening effect, as well as radiative heat exchange between the obstacle surface and incoming particles. Almost every problem of two phase heterogeneous flows is quite complex and computationally expensive due to the difference of characteristic scales for carrying and dispersed phases. There are two approaches to the numerical simulation of particle dynamics. The first one uses Eulerian description and treats admixture as continuous medium. The second one treats every particle in admixture independently and uses governing equations in Lagrangian variables. We use second approach, since it is more straightforward in simulation of consequent particle collisions with another particles and their reflections from the surface.

## 2 Discrete Trajectories and Discrete Element Methods

For given flow fields of carrying phase the dispersed phase dynamics is governed by partial differential equations in Lagrangian variables. Admixture particles are modeled as homogeneous isothermal hard spheres. The motion and heat transfer equations have the form:

$$m_p \frac{d\mathbf{v}_p}{dt} = \mathbf{f}_p, I_p \frac{d\boldsymbol{\omega}_p}{dt} = \mathbf{T}_\omega, c_{mp} m_p \frac{dT_p}{dt} = q_c + q_r$$

where  $m_p$  is mass,  $I_p$  – moment of inertia,  $T_p$  – temperature,  $\mathbf{v}_p$  – velocity,  $\boldsymbol{\omega}_p$  – angular velocity,  $c_{mp}$  – heat capacity of particle’s material,  $\mathbf{f}_p$  – external forces,  $\mathbf{T}_\omega$  – torque,  $q_c$  and  $q_r$  – convective and radiative heat fluxes respectively. Integrating these equations one yields stream lines for the discrete trajectories method and individual particle trajectories

for the discrete element method. In the first method admixture propagates from inflow to outflow boundaries with constant concentration discharge rate along the stream lines. In the second method each computational particle travels independently and can participate in unsteady unique events, such as interparticle collisions.

The discrete element method is much more computationally consuming than its steady counterpart since it requires not just single particle per stream line, but regular inflow of particles to maintain the specified admixture volume concentration at the inlet. To simulate interparticle collisions on every computational step  $[t^n; t^{n+1}]$  one constructs a trajectory approximation for each particle as the polynomial  $\mathbf{r}(t) = \mathbf{r}_2 t^2 + \mathbf{r}_1 t + \mathbf{r}_0$ . The condition for collision of pairs of particles  $i$  and  $j$  is expressed by the equation  $|\mathbf{r}_i(t) - \mathbf{r}_j(t)|^2 = (r_{pi} + r_{pj})^2$ , where  $r_{pi}$ ,  $r_{pj}$  are particles' radii.

### 3 Direct Collisions Simulation and Monte-Carlo method

The most accurate solution can be obtained by using an authors' full-scale version of the discrete element method [1], where each computational particle stands for a single real one. Parameters of paired interparticle encounters and collisions with an obstacle surface are computed using the above-said polynomial trajectory approximation. All particle impacts during one computational step  $[t^n; t^{n+1}]$  are simulated sequentially in chronological order using the queue of collisions. Parameters for a pair of particles after collision as well as particle properties after reflection from a surface are calculated according to the model of hard spheres [3]. Processing of each collision event removes all subsequent encounters for this particle from the queue. Then one obtains particle parameters after collision at the instant  $\tau \in (t^n; t^{n+1}]$ , proceeds to integration of equations of movement and heat exchange on the interval  $(\tau; t^{n+1}]$ , approximates new trajectory and computes parameters for new collisions. Newly found encounters are placed in the global queue and treated in a consistent chronological order. It is necessary to put all collisions in the queue, not just the first one, since some of them, including early ones can be removed as not happened. This algorithm continues until the encounter queue is empty on the current computational step.

This approach allows to simulate complex heterogeneous flows with the best accuracy, including repeated mutual collisions of particles and their reflection from the obstacle surface. However, the implementation of this method involves considerable computational cost and parallelization is possible only for solving movement and heat equations. Collisions in the queue are handled sequentially and generally unsuitable for parallel processing. Therefore such numerical treatment of interparticle collisions is very computationally expensive.

There are means to decrease computational costs for interparticle collisions and speed up simulation via some loss of spatial detalization for admixture. Two existing approaches are based on assumptions allowing to scale up particle dynamics from a single real particle to a group of them. Further simplification trades history of collisions for each computational particle on every timestep to random trials thus excluding unique deterministic trajectories and introducing stochastic averaged ones.

First approach to reduce the demands of discrete element method for computational resources is to represent every  $F$  real particles by a single probe particle. The probe particle has physical characteristics of a single particle when solving the equations of motion and simulating interactions with other particles. One should take into consideration the factor  $F$  for obtaining integral properties, such as an action of admixture on a carrier gas or an obstacle surface, or kinetic energy dissipation due to inelastic colli-

sions. To preserve the properties of the dispersed phase it is necessary to ensure that a probe particle has the same intensity of collisions along the trajectory, as a single real particle has. Therefore, the equation that determines the conditions of collision for a pair of probe particles is  $|\mathbf{r}_i(t) - \mathbf{r}_j(t)|^2 = (r_{pi}\sqrt{F} + r_{pj}\sqrt{F})^2$ . The results are the moments of time when a distance between centers of mass of the probe particles equals  $r_{pi}\sqrt{F} + r_{pj}\sqrt{F}$ . Parameters of particle pairs after collision are computed using a normalized vector defining the relative positions of the particles at the instance of the impact:  $\mathbf{n}_{ij} = (r_{pi} + r_{pj}) (\mathbf{r}_j(\tau) - \mathbf{r}_i(\tau)) |\mathbf{r}_j(\tau) - \mathbf{r}_i(\tau)|^{-1}$

The distinctive feature of the direct collisions simulation algorithm is an essentially consequent way of processing the queue of collisions. Parallelization is straightforward to implement only for integration of equations of movement and heat exchange at each computational time step. At the same time the computational costs reduce nonlinearly at the stage of collisions simulation increasing the integration step expences in overall costs, which means the increase of parallelization efficiency for the problem solution in whole. Figure 1 shows plots of the computer time costs versus the factor  $F$  for solving the problem in quasi-3D formulation. One can see that implementation of probe particles in combination with parallel computing reduces runtime up to a factor 10 while retaining the accuracy of full-scale solution (see Fig. 2). The problem was solved using PC based on Intel Xeon CPU with 4 cores.

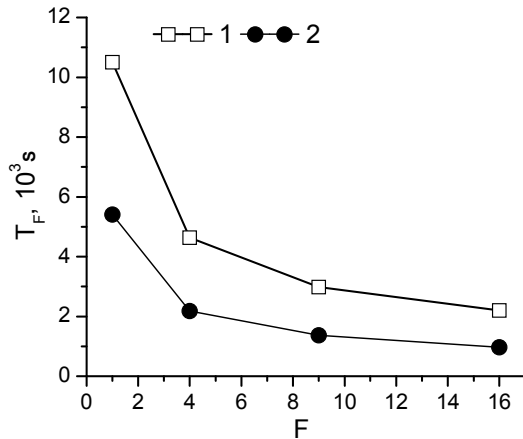


Figure 1: Runtime costs for the algorithms: 1 - successive, 2 - parallel

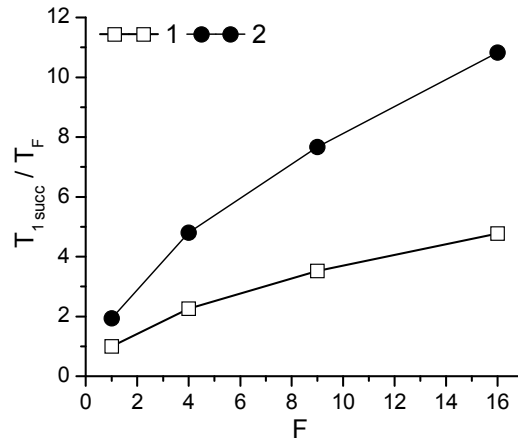


Figure 2: Runtime reduction for the algorithms: 1 - successive, 2 - parallel

Second approach to reduce computational costs is to use stochastic Direct Simulation Monte-Carlo methods (DSMC), e.g. [2]. In these methods particle dynamics on every timestep  $[t^n; t^{n+1}]$  is simulated via consecutive advection and collision stages. On collision stage computational domain  $U$  is split into nonintersecting cells  $U = \bigcup_{m=1}^M U_m$ . All particles contained in a one cell undergo statistical trials for possible collisions. A variety of Monte-Carlo methods is provided in [2, 4, 5]. We use one of the most popular variant of DSMC without time counter (No Time Counter, NTC) [2] with the following algorithm:

1. Compute the number of trials for collisions.  $P_m = F \frac{N_m^n (N_m^n - 1)}{2} \frac{v_{max}}{V_m} (t^{n+1} - t^n)$ , where  $v_{max} = \max_{i,j} v_{ij}$  for all particles  $i$  and  $j$  in the cell  $U_m$ ,  $v_{i,j} = \pi (r_{pi} - r_{pj})^2 |\mathbf{v}_i - \mathbf{v}_j|$ ,  $r_p$  - particle radius,  $\mathbf{v}$  - particle velocity,  $N_m^n$  - number of particles in the cell,  $V_m$  - cell volume,  $F$  - ratio between real and computational particles.
2. Proceed trials  $P_m$  times. On each trial select equiprobably a pair of particles  $p_i$  and  $p_j$  from cell  $U_m$ , then compute  $v_{ij}$ . Generate random number  $\beta$ , uniformly distributed

on  $[0; 1]$ . If  $\beta < \frac{v_{ij}}{v_{max}}$  then simulate a collision, otherwise proceed with next trial. In case of collision compute vector of relative positions  $\mathbf{n}_{ij}$  and if particles are closing-in  $\mathbf{n}_{ij}(\mathbf{v}_j - \mathbf{v}_i) < 0$  then change their parameters according to the model of collision.

There are several approaches to calculation of  $\mathbf{n}_{ij}$  in literature:

1. Vector  $\mathbf{n}_{ij}$  connects particles mass centers  $\mathbf{n}_{ij} = (r_{pi} + r_{pj}) \frac{\mathbf{r}_j - \mathbf{r}_i}{|\mathbf{r}_j - \mathbf{r}_i|}$ .

2. Vector direction is randomly uniformly distributed in space:

$\mathbf{n}_{ij} = (r_{pi} + r_{pj}) (\mathbf{i} \cos \chi + \mathbf{j} \sin \chi \cos \epsilon + \mathbf{k} \sin \chi \sin \epsilon)$ , where  $\cos \chi = 2\beta - 1$ ,  $\sin \chi = \sqrt{1 - \cos^2 \chi}$ ,  $\epsilon = 2\pi\alpha$ ,  $\alpha$  and  $\beta$  are uniformly distributed on  $[0; 1]$ .

3. Projection  $\mathbf{b}$  of vector  $\mathbf{n}_{ij}$  on the plane orthogonal to relative velocity vector  $\mathbf{v}_j - \mathbf{v}_i$  is distributed on  $[0; r_{pi} + r_{pj}]$  proportionally  $|\mathbf{b}|$  [2]:

$\mathbf{n}_{ij} = (r_{pi} + r_{pj}) (\mathbf{i}'' \cos \chi + \mathbf{j}'' \sin \chi \cos \epsilon + \mathbf{k}'' \sin \chi \sin \epsilon)$ , where  $\cos \chi = \sqrt{\beta}$ ,  $\sin \chi = \sqrt{1 - \cos^2 \chi}$ ,  $\epsilon = 2\pi\alpha$ ,  $\alpha$  and  $\beta$  are uniformly distributed on  $[0; 1]$ . Coordinate system  $0x''y''z''$  is yielded by rotation of initial system  $0xyz$ , so that axis  $0x''$  becomes collinear with vector of relative velocity :  $i'' = \frac{\mathbf{v}_j - \mathbf{v}_i}{|\mathbf{v}_j - \mathbf{v}_i|}$

The DSMC variants are quite feasible for molecular dynamics simulation; however in case when gradients of particles concentration are large, statistical methods suffer from a loss of accuracy.

## 4 Results and Discussion

First, we consider a computational experiment for chaotically moving particles without carrying gas phase. At initial moment computational domain is filled with monosized particles uniformly distributed in space. Their velocity lengths are equal, and velocity directions are distributed uniformly. Domain has periodical boundary conditions. In general case particle collisions are inelastic. Distributions of collisions number against angle are shown on Fig. 3. This angle is the angle between vector of relative velocity and vector connecting particle mass centers at an instant of collision. First and second variants for vector  $\mathbf{n}_{ij}$  yield similar results, yet they have qualitative differences from solutions, obtained by precise simulation and DSMC with the third variant of relative position vector  $\mathbf{n}_{ij}$ . The collisions number  $N_a$  is non-dimensionalized by the number of particles entering computational domain through unit of surface per unit of time  $N_s$ . Dissipation of kinetic energy  $E_{Kdisp}$  is scaled to summary kinetic energy of particles at the inflow  $E_{K0}$  (Fig. 4).

Next we consider a problem of supersonic heterogeneous flow over a sphere. Gas phase is governed by a system of modified Euler equations. Gasdynamics equations are integrated numerically via HLL scheme. Boundary conditions for a solid curvilinear surface are approximated according to the ghost-cell immersed boundary method on rectangular grids. Parameters of a gas phase represent the atmospheric conditions at 10 km; Mach number  $M_\infty = 6$ . Admixture is represented by particles  $10 \mu m$  in diameter of aluminum dioxide  $Al_2O_3$ . Volume concentration for admixture is  $C_{V0} = 10^4$ . Sphere radius is 3 cm. It's necessary to note that regardless of axial symmetry for carrying gas flow, admixture simulation should be proceeded in three dimentions. To reduce computational costs for the full-scale discrete element method we used probe particles with various values of factor  $F$ .

Figures 5-7 show dynamical and energetical impact of admixture on the sphere surface in the case of inelastic interparticle collisions. Velocity restitution coefficient for hard spheres model was defined equal to 0.5. One can see that DSMC yields lower intensity of particle-surface collisions and, correspondingly, higher averaged particle normal velocity at the moment of collision with the surface (see Fig 5-6). Intensity of collisions is related to

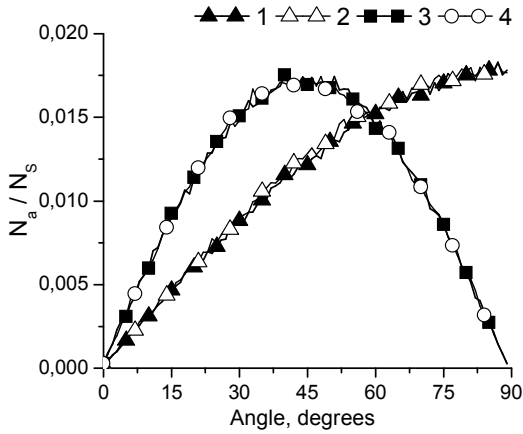


Figure 3: Distribution of collisions number vs. angle between vector of relative velocity and vector connecting particle mass centers at an instant of collision. 1-3 – DSMC, 4 – reference simulation by the full-scale discrete element method.

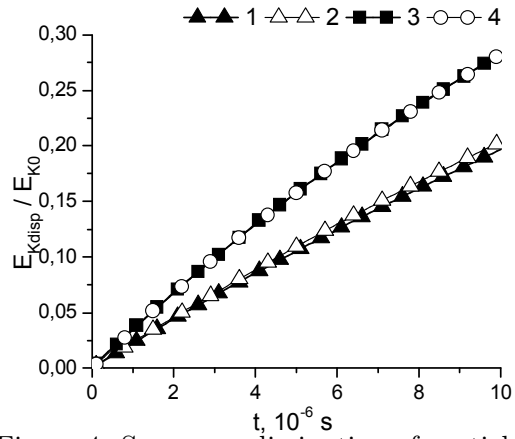


Figure 4: Summary dissipation of particles kinetic energy due to inelastic collisions. 1-3 – DSMC, 4 – reference simulation by the full-scale discrete element method.

intensity of inflow particles  $I_\infty$  and averaged normal velocity  $V_N$  is scaled to particle free stream velocity  $V_\infty$ .

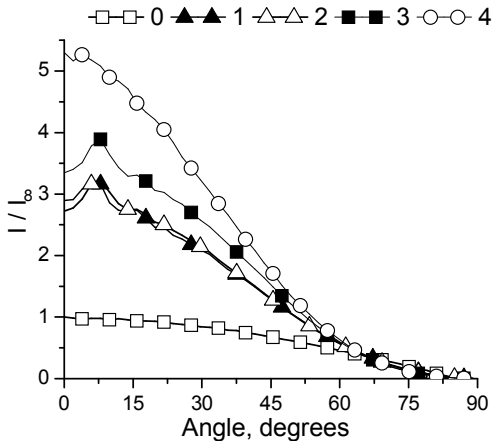


Figure 5: Intensity of particle collisions with the sphere surface. 0 – Discrete trajectory method without interparticle collisions, 1-3 – DSMC, 4 – reference simulation by the full-scale discrete element method.

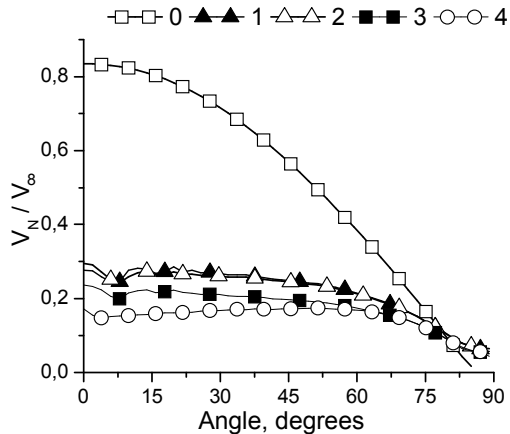


Figure 6: Averaged value of particle normal velocity at an instant of collision with the sphere surface. 0 – Discrete trajectory method without interparticle collisions, 1-3 – DSMC, 4 – reference simulation by the full-scale discrete element method.

The screening effect can be observed. It arises due to some kinetic energy dissipation for incident particles colliding with reflected ones and leads to lower impact of admixture on the surface. First and second variants for  $\mathbf{n}_{ij}$  in DSMC give less intensive kinetic dissipation (see Fig. 4), what leads to underestimation of the screening effect compared to the reference results of the full-scale discrete element method. Third variant of  $\mathbf{n}_{ij}$  is in close agreement with the accurate solution (see Fig. 7). The main drawback of all Monte-Carlo methods is that they prone to underestimate the number of subsequent collisions in the areas with strong macroscopic gradients of admixture concentration (Fig. 8) and

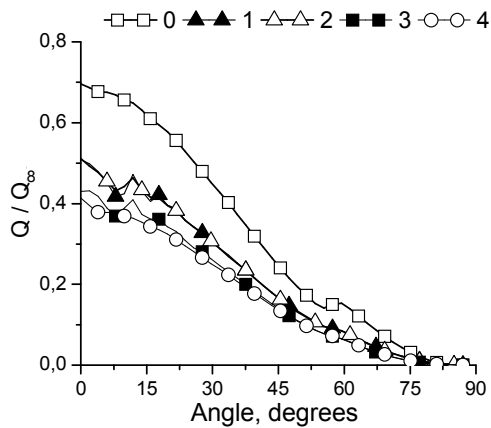


Figure 7: Energy flux density from admixture to the surface of the sphere. 1-3 – DSMC, 4 – reference simulation by the full-scale discrete element method.

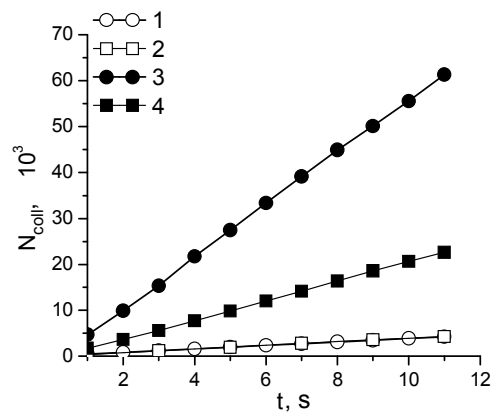


Figure 8: Summary number of interparticle collisions. 1, 2 – away from the surface ( $d > 0.02R$ ), 3, 4 – in the vicinity of the surface ( $d \leq 0.02R$ ). 2, 4 – DSMC, 1, 3 – reference simulation by the full-scale discrete element method. Here  $d$  – distance from particle to the obstacle surface,  $R$  – sphere radius.

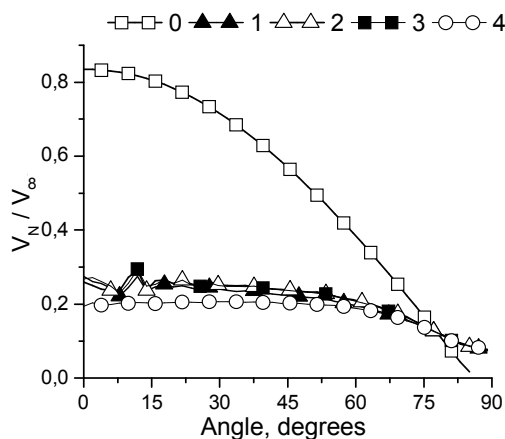


Figure 9: Averaged normal velocity component for a particle at an instant of collision with the surface. 0 – Collisionless simulation, 1-3 – DSMC, 4 – reference simulation by the full-scale discrete element method. Interparticle collisions are absolutely elastic.

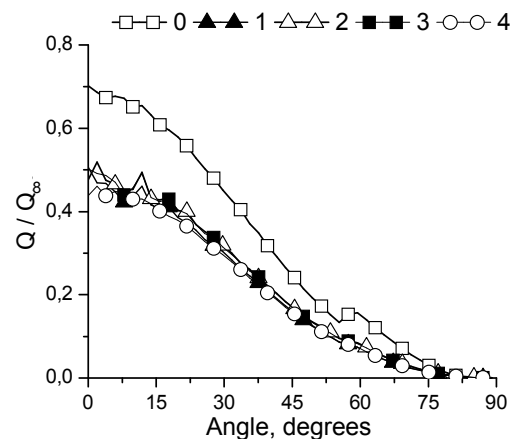


Figure 10: Summary dissipation of particles kinetic energy due to inelastic collisions. 1-3 – DSMC, 4 – reference simulation by full-scale discrete element method. Interparticle collisions are absolutely elastic.

so misrepresent dynamic action of admixture on the surface (see Fig. 5,6). Regardless of these numerical qualities the integral parameters such as energy flux density (Fig. 7) yielded by the third DSMC method are quite accurate. It can be explained by the fact that the maximum energy dissipation occurs for the first collisions at high relative velocities. Represented energy flux density is scaled to  $Q_\infty$  – energy flux density for free stream particles.

Similar computations were carried out for a case of absolutely elastic interparticle collisions. The plots for dynamical and energy impact of admixture on a surface are shown on Fig. 9-10. One can see that the differences between various DSMC methods are nearly

vanish, since there is no kinetic energy dissipation in such collisions. In this case the screening effect arises only due to change of velocity direction for incident particles colliding with reflected ones.

## Conclusions

Two approaches to numerical simulation of collisional dynamics of dispersed admixture in heterogeneous flows are discussed, namely direct full-scale discrete element numerical simulation and statistical Monte-Carlo simulation. Implementation of probe particles in the discrete element method significantly extends application area by reducing demands for computer memory and runtime allowing to implement parallel computing algorithms. Therefore modifications of discrete-element method make numerical simulation of three-dimensional dusty flows past an obstacle quite plausible. It is shown that the DSMC method used for the problem of heterogeneous flow over the obstacle yields correct and accurate integral parameters of admixture impact on the surface such as particles energy flux density to the obstacle.

## Acknowledgements

*The work is supported by RFBR grant No 12-08-00867 and President's grant for support for young Russian scientists MK-179.2011.8.*

## References

- [1] Reviznikov D.L. and Sposobin A.V. Direct numerical modeling of disperse phase flow of gas-particle mixture over a body [in Russian]// e-journal “Trudy MAI”, 2007, No.26, 13 p.
- [2] Bird G. A. Molecular Gas Dynamics and the Direct Simulation of Gas Flows. // New York, Oxford, Clarendon Press, 1994, 476 p.
- [3] Crowe C.T., Sommerfeld M. and Tsuji Y. Multiphase flows with droplets and particles. CRC Press LLC, 1998, 471 p.
- [4] Bird G. A. Sophisticated DSMC. // Proceedings of the Notes from a short course held at the DSMC07 Conference, Santa Fe, USA, 2007.
- [5] Volkov A.N., Tsirkunov Yu.M. CFD / Monte Carlo simulation of collision-dominated gas-particle flows over bodies. // Proceedings of ASME 2002 Fluids Engineering Division Summer Meeting, Montreal, Quebec, Canada, July 14-18, 2002.
- [6] Mikhatulin D.S., Polezhaev Yu.V., Reviznikov D.L. Heat exchange and destruction of bodies in supersonic heterogeneous flows. [in Russian]. Moscow, Janus-K, 2007, 392 p.
- [7] Vinnikov, V. and Reviznikov, D. and Sposobin, A. Two-phase shock layer in a supersonic dusty gas flow // Mathematical Models and Computer Simulations, 2010, Vol. 2, No. 4, pp. 514–525.

*Vladimir V. Vinnikov, Moscow Aviation Institute, Volokolamskoe sh. 4, 125993, Moscow, Russia  
Dmitry L. Reviznikov, Moscow Aviation Institute, Volokolamskoe sh. 4, 125993, Moscow, Russia  
Andrew V. Sposobin, Moscow Aviation Institute, Volokolamskoe sh. 4, 125993, Moscow, Russia*